Structural model of human GAD65: Prediction and interpretation of biochemical and immunogenic features

ARTICLE *in* PROTEINS STRUCTURE FUNCTION AND BIOINFORMATICS · APRIL 2005

Impact Factor: 2.63 · DOI: 10.1002/prot.20372 · Source: PubMed

5 AUTHORS, INCLUDING:

Daniela De Biase
Sapienza University of Rome
50 PUBLICATIONS **1,301** CITATIONS

SEE PROFILE

Structural Model of Human GAD65: Prediction and Interpretation of Biochemical and Immunogenic Features

Guido Capitani,[1]* Daniela De Biase,[2,3] Heinz Gut,[1] Shaheen Ahmed,[1] and Markus G. Grütter[1]
[1]*Biochemisches Institut der Universität Zürich, Zürich, Switzerland*
[2]*Dipartimento di Scienze Biochimiche, Università di Roma La Sapienza, Roma, Italy*
[3]*Centro di Eccellenza di Biologia e Medicina Molecolare, Università di Roma La Sapienza, Roma, Italy*

ABSTRACT **The 65 kDa human isoform of glutamate decarboxylase, GAD65, plays a central role in neurotransmission in higher vertebrates and is a typical autoantigen in several human autoimmune diseases, such as insulin-dependent diabetes mellitus (IDDM), Stiff-man syndrome and autoimmune polyendocrine syndrome type I. In autoimmune diabetes, an attack of inflammatory cells to endocrine pancreatic β-cells leads to their complete destruction, eventually resulting in the inability to produce sufficient insulin for the body's requirements. Even though the etiology of β-cell destruction is still a matter of debate, the role and antigenic potency of GAD65 are widely recognized. Herein a model of GAD65 is presented, which is based on the recently solved crystal structures of mammalian DOPA decarboxylase and of bacterial glutamate decarboxylase. The model provides for the first time a detailed and accurate structure of the GAD65 subunit (all three domains) and of its dimeric quaternary assembly. It reveals the structural basis for specific antibody recognition to GAD65 as opposed to GAD67, the other human isoform, which shares 81% sequence similarity with GAD65 and is much less antigenic. Literature data on monoclonal antibody binding are perfectly consistent with the detailed features of the model, which allows explanation of several findings on GAD65 immunogenicity. Importantly, by analyzing the active site, we identified the residues most likely involved in catalysis and substrate recognition, paving the way for rational mutagenesis studies of the GAD65 reaction mechanism, specificity and inhibition. Proteins 2005;59:7–14.**

Key words: diabetes; GAD65; GABA; neurotransmission; autoimmune diseases; antibody binding; epitope mapping; homology modeling; structure prediction

INTRODUCTION

Glutamate decarboxylase (GAD, E.C. 4.1.1.15) catalyzes the irreversible α-decarboxylation of L-glutamate to γ-aminobutyrate (GABA). GAD is a pyridoxal 5′-phosphate (PLP)-dependent enzyme and is widely distributed among eukaryotes and prokaryotes.[1] In the central nervous system of higher vertebrates, GAD is recognized as a key enzyme because glutamate, its substrate, and GABA, its product, are the major excitatory and inhibitory neurotransmitters, respectively.[2] GAD activity, which is already detectable at the embryonic stage in rat cerebral cortex and increases significantly during the second postnatal week, always precedes the appearance of GABAergic synapses, strongly indicating an important role of this enzyme in neuronal development.[3] GABA is involved in most of the integrative functions of the brain, and several neurological and psychiatric disorders originate from an impaired transmission through GABAergic neurons.[4] Moreover, GABA and GAD are present in several non-neuronal tissues,[5] including the pancreatic β-cells from which GABA is released to regulate glucagon secretion by pancreatic α-cells.[6] In most vertebrate classes, GAD occurs in two non-allelic isoforms, GAD65 and GAD67, which originated by a gene duplication event that occurred between 400 and 560 million years ago.[7] Human GAD67 and GAD65 genes share a common intron–exon boundary and are localized to chromosomes 2 and 10, respectively.[8–10] The 3.7 kb human GAD67 mRNA encodes a 594-residue, hydrophilic, soluble polypeptide that is found mainly in the cell bodies of neurons and in the cytosol of pancreatic β-cells.[11,12] The 5.6 kb human GAD65 mRNA encodes a 585-residue polypeptide having a sequence 65% identical and 81% similar to that of GAD67.[9] GAD65 is more hydrophobic and less soluble than GAD67 because of post-translational modifications and significant sequence differences primarily located towards the N-terminus, which is reversibly anchored to membranes in synaptic vesicles of neurons and synaptic-like microvesicles in pancreatic β-cells.[13,14] Both GAD isoforms are active at neutral pH as dimers.[1] Experiments in knockout mice and in rats treated with vigabatrin, an inhibitor of the GABA-catabolizing enzyme GABA-transaminase, indicate that GAD67 is sufficient for most GABA synthesis in the brain and that the two isoforms are not fully interchangeable.[15,16] In fact, GAD65

Abbreviations: GAD, glutamate decarboxylase; GABA, γ-aminobutyrate; DDC, DOPA decarboxylase; GadB, glutamate decarboxylase isoform B from *Escherichia coli*; PLP, pyridoxal 5′-phosphate

*Correspondence to: Guido Capitani, Biochemisches Institut der Universität Zürich, Zürich CH-8057, Switzerland. E-mail: capitani@bioc.unizh.ch

Received 27 July 2004; Revised 30 August 2004; Accepted 30 August 2004

Published online 2 February 2005 in Wiley InterScience (www.interscience.wiley.com). DOI: 10.1002/prot.20372

not only cannot compensate for the loss of GAD67, but it is mainly present as the apo-enzyme, which becomes readily activated upon PLP supply, when additional GABA production is needed.[17] Notably, GAD65 is the primary GAD isoform expressed in human pancreatic β-cells[8] and has been recognized as a major autoantigen involved in progressive destruction of these cells, eventually leading to the development of insulin-dependent diabetes mellitus (IDDM).[18] In this illness, a T-cell-mediated attack of the immune system destroys pancreatic β-cells, and GAD65 autoantibodies are an early marker of the disease.[19] Several studies have been carried out in order to identify which epitopes on the surface of GAD65 are recognized by the autoantibodies.[20–24] Anti-GAD65 antibodies are also present in other autoimmune diseases, such as Stiff-man syndrome[25] and Batten disease.[26] In the case of Batten disease, the autoantibody appears to inhibit glutamate decarboxylase activity, resulting in abnormally high levels of glutamate in the brain.[26]

Detailed structural information on GAD65 has been long sought after in order to rationalize findings from epitope mapping experiments, plan mutagenesis experiments and understand the biochemical features of this enzyme. Several earlier attempts to construct homology models have been limited by the absence of available experimental structures with strong similarity to GAD65.[20,23,27] The situation changed recently, when the crystal structures of pig kidney DOPA decarboxylase (DDC)[28] and of *Escherichia coli* glutamate decarboxylase isoform B (GadB)[29] were solved. Both proteins share moderate but significant sequence similarity with GAD65 and together provide sufficient information for a high-quality structural model of GAD65.

MATERIALS AND METHODS

Structural Alignment of GadB and DDC

The crystal structures of DDC from *Sus scrofa* [Protein Data Bank (PDB) entry 1JS3][28] and GadB from *Escherichia coli* at low pH (active form, PDB entry 1PMM)[29] were superimposed using the program O.[30] For DDC, the superposition was carried out on the entire dimer; for GadB, which is a hexamer, subunits A and B were chosen. The corresponding structural alignment was used as a seed for a multiple sequence alignment (MSA) encompassing other sequences sharing high similarity to either pig DDC or *E. coli* GadB. The sequence of human GAD65 was then inserted in this MSA, taking into account information from a sequence-based multiple alignment of all aforementioned sequences, performed with PILEUP (GCG)[31] and manually corrected by aligning the observed secondary structural elements of pig DDC and GadB with those predicted for GAD65 by the program JPRED.[32]

Homology Modeling of GAD65

The final alignment of the GAD65 sequence with the subunit sequences of pig DDC and *E. coli* GadB was duplicated to simulate a dimer. The alignment was then fed into the program MODELLER,[33] using the 1JS3 dimer and the selected A,B dimer from 1PMM as structural templates. The PLP cofactor was treated as a rigid body in this phase. A total of 99 homology models was generated, with symmetry restraints on the two subunits to keep the dimer symmetric. Following indications from secondary structure prediction, additional restraints were added to keep residues 412–420, 423–426 and 519–538 in α-helical conformations. The resulting models were evaluated for stereochemical quality using the program PROCHECK.[34] The best was energy-minimized using X-PLOR 3.851[35] with the topology and parameter files TOPH19.PRO and PARAM19.PRO. The geometry of the internal aldimine linkage between Lys396 and the cofactor was optimized in this phase. The structure was validated with WHAT_CHECK.[36]

RESULTS AND DISCUSSION

Structure Quality

The present GAD65 model exhibits excellent stereochemical quality, with 87.8% of the residues in the most favored region, 10.6% in the additionally allowed region, 1.6% in the generously allowed region and no residue in the disallowed regions of the Ramachandran plot. Validation results using WHAT_CHECK[36] were similar to those expected for a low-resolution crystallographic structure. The model coordinates are available from the authors.

Subunit Structure

The final model of the GAD65 homodimer exhibits the features of a typical PLP-dependent enzyme of fold type I [37] with the two subunits related by a twofold axis and sharing a rather large dimer interface (Fig. 1), which amounts to ≈5200 Å^2. This value is comparable to the ≈5700 Å^2 interface for native DDC (PDB code 1JS6). Since the model of each GAD65 monomer (Fig. 2) encompasses residues from Gly103 to Arg128 and from Leu141 to Leu585, the dimer interface area for full-length GAD65 is probably even larger than 5200 Å^2. As described in Materials and Methods, the model was constructed using *Sus scrofa* DDC (1JS3) and *E. coli* GadB (1PMM) as templates, which, on the basis of the structural alignment shown in Figure 3, share 19% and 12% sequence identity with GAD65, respectively. No attempt was made to model the N-terminal region comprising the first 102 residues in GAD65, for which secondary structure prediction with PSIPRED[38] indicates 5 α-helices. The difficulty in aligning this region with other decarboxylases of known structure is easily explained by the peculiar functions associated to this GAD65 portion, not typical of PLP-dependent enzymes. This region, which targets GAD65 to the Golgi compartment and to the presynaptic clusters,[39] is difficult to model because a corresponding region does not exist in the amino acid decarboxylases of known structure.

Having excluded the 102-residue N-terminal segment from the model, three domains are evident in the GAD65 monomer structure (Fig. 2). In GadB and DDC, as in other enzymes from the same family, these are referred to as the N-terminal domain, the large domain and the small domain. We will use the same terminology for our model of GAD65 while recognizing that the N-terminal domain

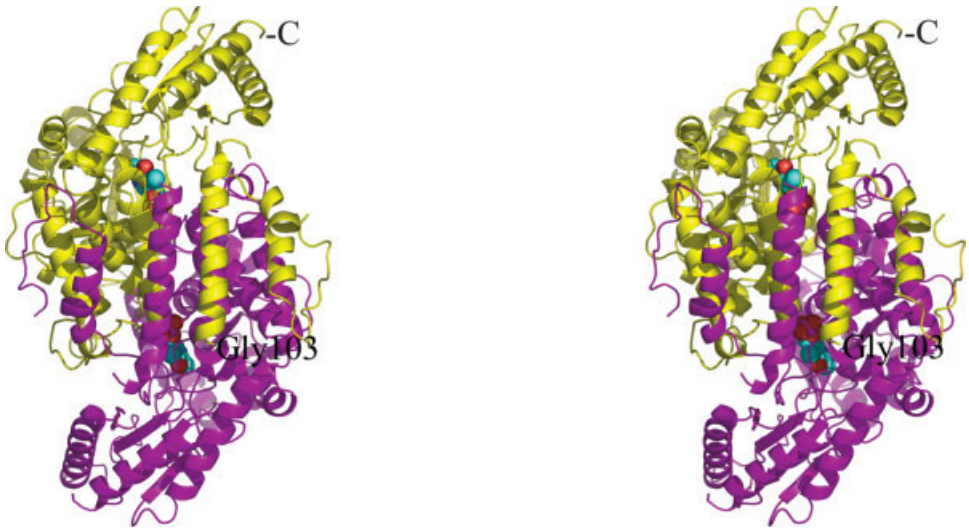

Fig. 1. Stereo cartoon representation of the GAD65 model, with the two subunits depicted in yellow and magenta. The cofactor molecules appear in space-filled representation. Prepared with Pymol (www.pymol.org).

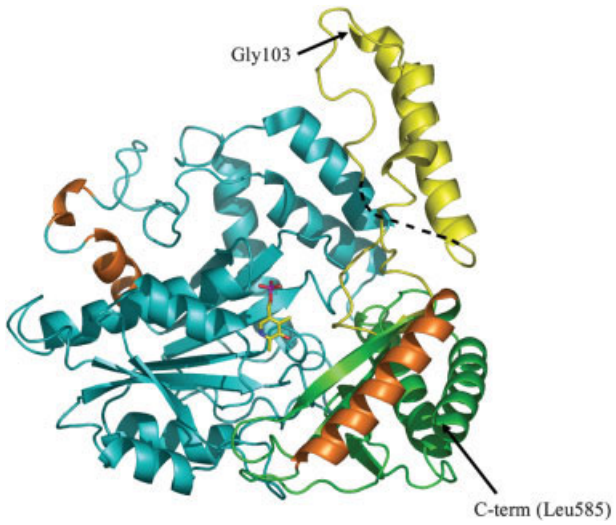

Fig. 2. Subunit structure of GAD65 in cartoon representation. The N-terminal domain (residues 103–128 and 141–187) appears in yellow, the large domain (residues 188–464) in cyan and the small domain (residues 465–585) in green. The cofactor is in ball-and-stick representation. Residues restrained to α-helical conformation appear in dark orange. Prepared with Pymol.

referred to is not the true N-terminus. In the present model, only residues 103–128 and 141–187 constitute the GAD65 N-terminal domain, which was modeled based mainly on the DDC N-terminal domain (DDC residues 1–85[28]). As in DDC, the N-terminal domain of each monomer contributes considerably to the dimer interface (Fig. 1). The large domain of the GAD65 model (residues 188–464) contains the cofactor binding site, consisting of an α/β-fold made of a central seven-stranded mixed β-sheet surrounded by eight α-helices, typical of PLP-dependent enzymes belonging to type-I folds.[40] In the DDC crystal structure, residues 328–339, corresponding to the 421–432 stretch in GAD65, are not visible, due to disorder or to proteolysis. The structurally equivalent region of GadB (residues 300–313), which forms a β-hairpin narrowing the active site funnel of the other subunit in the dimer and taking part in the pH-dependent control of substrate accessibility, does not align well with residues 421–432 in the GAD65 sequence. Thus, in the absence of a suitable template, the 421–432 region of GAD65 was modeled according to secondary structure prediction with PSIPRED.[38] The conformation of this region (Fig. 2) is therefore less reliable than that of the remainder of our model.

The small domain of the GAD65 model (residues 465–585) consists of a four-stranded antiparallel β-sheet with three helices packed against the face opposite the large domain and closely resembles its DDC counterpart.

The Active Site

The model of GAD65 provides detailed information about the active site of the protein, which is more similar to that of DDC than to that of GadB. Several active site residues are conserved. They occupy structurally equivalent positions in the GAD65 model and in both crystallographic structures. These are (GAD65, GadB and DDC numbering, respectively): Thr339(212)[246], Asp364(243)[271], Ala366(245)[273], His395(275)[302], Lys396(276)[303] and Arg558(422)[447]. Figure 4 shows the active site of GAD65. In both GAD65 and DDC, the pyridine ring of the PLP is sandwiched between an alanine and a histidine residue (Ala366 and His282 in GAD65, Ala273 and His192 in DDC), whereas in the GadB active site the PLP is sandwiched between Ala245 and Gln163, structurally equivalent to His282 in GAD65. The PLP phosphate is anchored to the proteins in similar but not identical ways: in GAD65 the phosphate-binding site comprises a free cysteine residue from the other subunit (Cys446*), which corresponds to Gly354* in DDC. Oxidation of Cys446* may compromise PLP binding, consistent with the observation that antioxidants are essential to

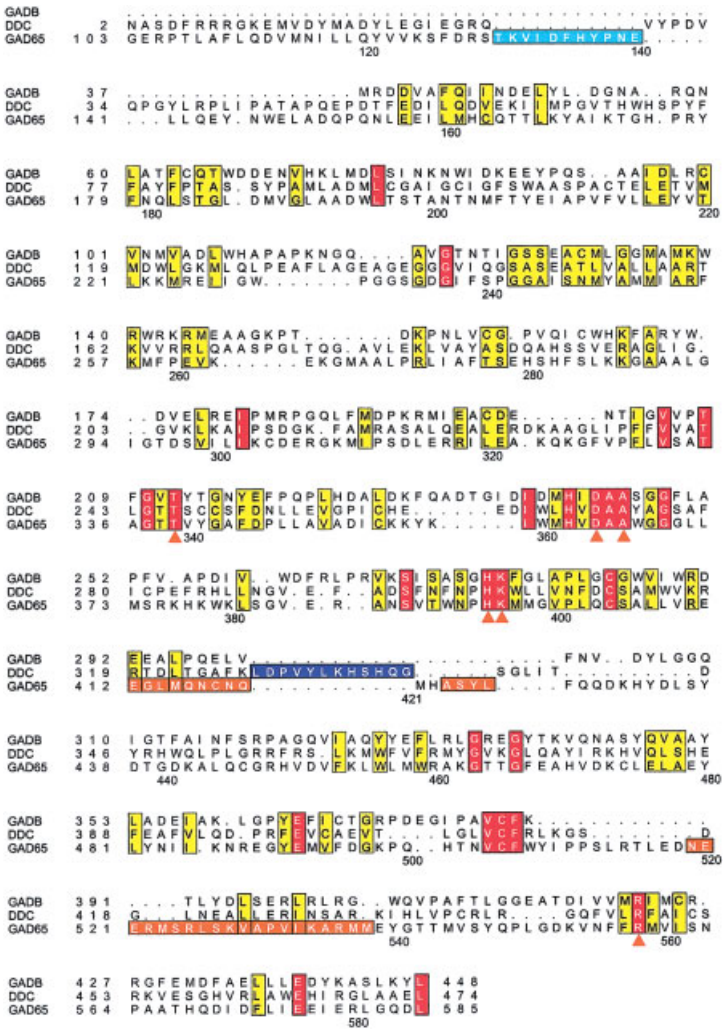

Fig. 3. Structural alignment of *E. coli* GadB, pig DDC and human GAD65 sequences. Strictly conserved residues are in red; highly conserved residues are in yellow. The cyan-boxed sequence refers to GAD65 residues 129–140, which were not modeled; the blue-boxed sequence refers to DDC (1JS3) residues 328–339 not visible in the crystal structure.[28] GAD65 residues that were restrained to assume an α-helical conformation, as deduced by PSIPRED, are boxed in orange. The active site residues conserved in GAD65, GadB and DDC are indicated by orange triangles.

maintain GAD at its maximal activity, probably due to the presence of oxidation-sensitive sulfhydryl groups.[41]

In all three active sites, an arginine residue, Arg558 in GAD65, is found at the same sequence and spatial position as the arginine that binds the α-carboxylate of the substrate in many PLP-dependent enzymes. However, in all three cases, the side chain of a hydrophobic residue prevents the guanidinium group of this arginine from binding the α-carboxylate of the corresponding amino acid substrate. In GAD65, the side chain of Leu182 keeps the guanidinium group of Arg558 away so that it cannot interfere with the α-decarboxylation of the substrate. Phe63 and Phe80 in GadB and DDC, respectively, play this role.[29]

In the modeled GAD65 dimer, the neighboring subunit contributes a residue, Asn203*, corresponding spatially to Ile101* in DDC, the side chain of which protrudes towards the region where the distal carboxylate of the substrate is supposed to bind. Thus, the carboxamide group of Asn203*, a residue conserved in all known metazoan glutamate decarboxylases, probably binds the distal carboxylate of the substrate glutamate. The nearby Phe205* is predicted to create a hydrophobic environment with its side chain as does the homologous Phe103* in DDC.[28] Interestingly, in *E. coli* GadB the neighboring subunit provides an aspartate residue (Asp86*), functionally and structurally similar to Asn203*, though its chemical nature is more compatible with the acidic pH optimum of bacterial Gad.[29] Chen et al.[42] report distinctive PLP-binding properties for GAD65 and GAD67. While the former exhibits a lower cofactor-binding constant, very similar for both active sites, the latter has higher affinity for PLP, with one active site binding the cofactor more tightly than the other. Mapping of the GAD67 sequence onto the GAD65 model shows that no mutations are found in the residues that bind and surround the cofactor in the active site. Thus, the differences in PLP-binding behavior between the two isoforms are to be explained by subtle structural differences, which affect PLP binding in an indirect way.

Autoantibodies to GAD65 are detected in several autoimmune diseases, such as IDDM, Stiff-man syndrome, polyendocrine syndrome type 1 and Batten disease.[19,25,26,43,44] Since the enzyme is so highly antigenic that it induces a similar T-cell proliferative response in IDDM patients and

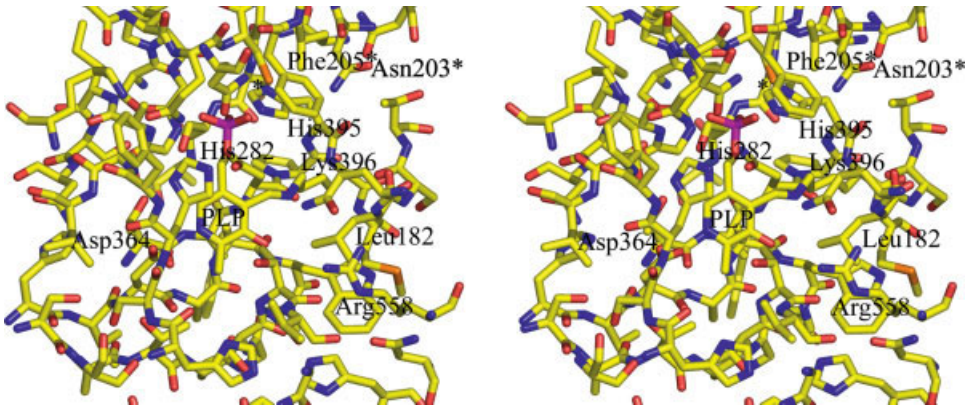

Fig. 4. Stereo ball-and-stick representation of the GAD65 active site in yellow and atom colors. The residue denoted by an asterisk is Cys446*. Prepared with Pymol.

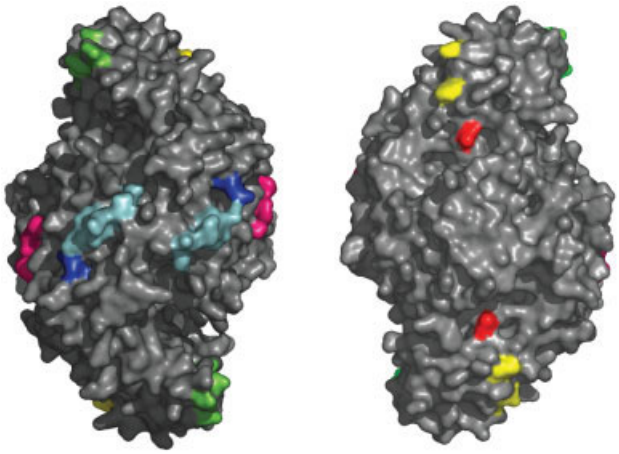

Fig. 5. Mapping of epitopes onto the surface of the Gad65 dimer, "front" (left) and "rear" (rotated by 180° along the *y*-axis, right) views. The following epitopes are mapped: M1, res. 483,568, yellow; M4, res. 358, blue; M5, res. 517,520,521,524,527, green; DPC, res. 231–234, hotpink; MICA3, res. 260–265, cyan; HLA-DR4, res. 557, 560,562,565, red. Prepared with Pymol.

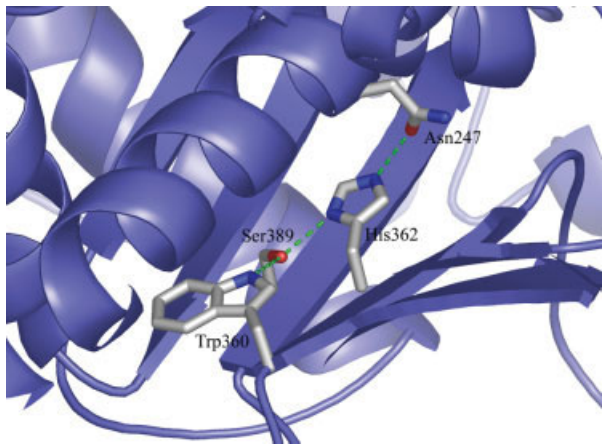

Fig. 6. Ball-and-stick representation of His362 and its environment, particularly its hydrogen-bonding interaction with Asn247. The protein backbone appears in cartoon representation. Prepared with Pymol.

normal subjects,[45] it is currently believed that T cell-mediated autoimmune destruction of the β-cells in the pancreatic Langerhans islets is triggered by a cross-reactive microbial antigen in a genetically susceptible host. This phenomenon is referred to as molecular mimicry and in the case of GAD65 is controversially attributed to different antigens: to residues 28–50 in the sequence of the P2-C coat protein of the Coxsackie B4 virus[21,23] and to the region encompassing residues 674–687 of the major DNA-binding protein of human cytomegalovirus.[46]

The availability of DDC and GadB as templates allowed us to overcome the limitations of previous homology models of GAD65[20,23,27] based mainly on the bacterial ornithine decarboxylase structure (1ORD),[47] which aligns poorly with the small domain of GAD65. The high-quality structural model of human GAD65 presented in this work represents a valuable tool because it reveals the structural basis for discrimination between GAD65 and GAD67 by specific antibodies and it provides an explanation of how single amino acid substitutions influence the relative antigenicities. Our model of dimeric GAD65 (Fig. 1) is clearly very different from a previously reported one,[20] in which the extensive dimer interface, reported in the present work and typical of fold-type I PLP-enzymes, is drastically reduced. Thus, the improvement in overall structural quality is due to the templates used, which allowed construction of the N-terminal domain (residues 103–187) and a more reliable modeling of the small domain. Figure 5 highlights the location of exposed amino acid residues in selected epitopes within a list computed from epitope mapping studies.[20,24,48] The model is perfectly consistent with specific reactivities described in the literature and sheds new light on several aspects of GAD65 antigenicity and folding behavior. First, Glu264 is a critical amino acid for the binding of antibody M10 and it is replaced by a threonine in GAD67. The Glu264–Thr mutation in GAD65 abolishes M10 reactivity.[20] Our model indicates that the side chain of Glu264 is totally exposed and protrudes from a short loop, which appears to be conformationally very well defined. Replacement of Glu264 with Thr is very unlikely to alter the loop conformation, so the critical factor for M10 monoclonal antibody binding

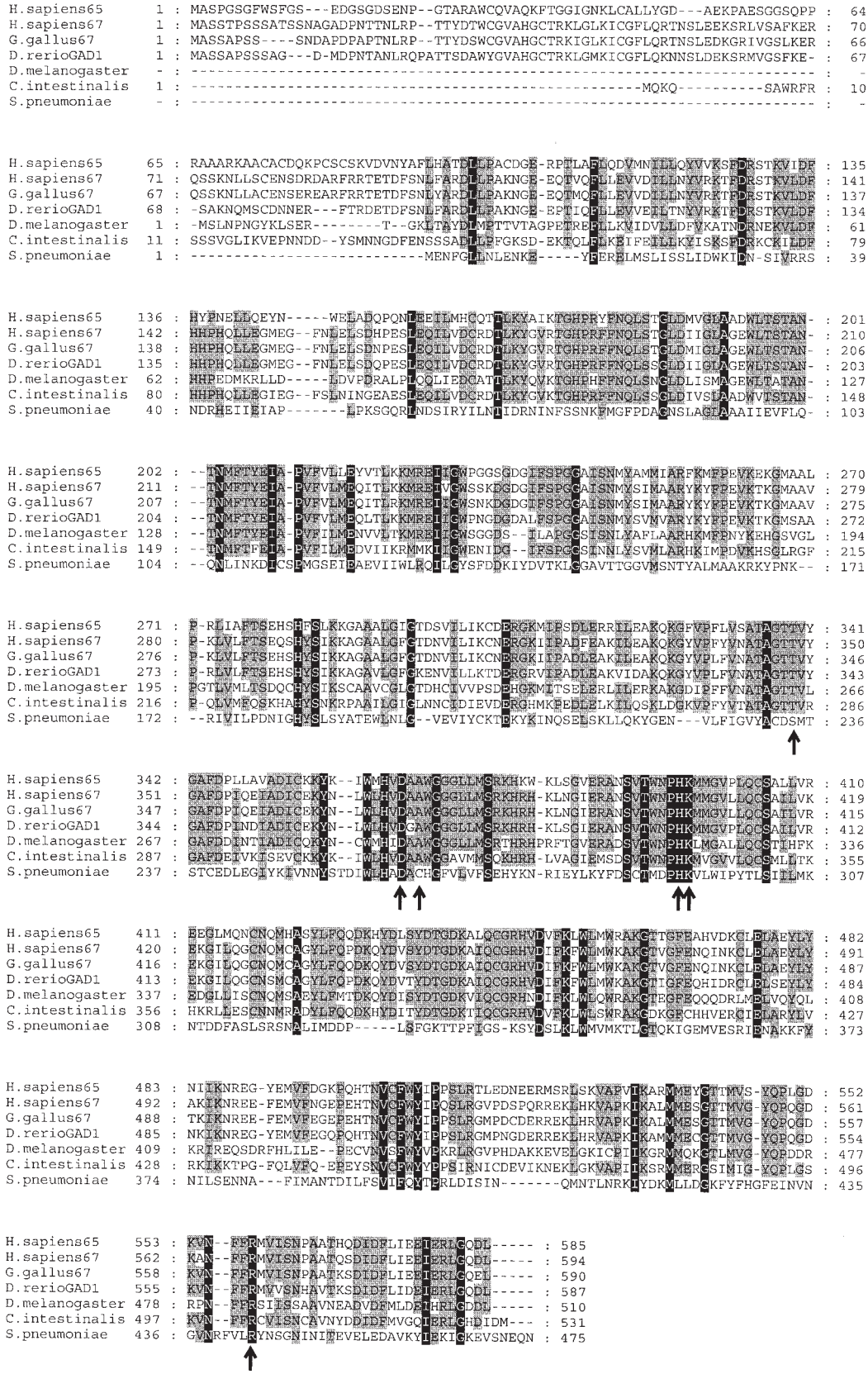

Fig. 7. MSA of six metazoan and of *S. pneumoniae* glutamate decarboxylases. The alignment was prepared with CLUSTALX.[52] Completely conserved residues are shaded black and partially conserved ones in gray. The active site residues conserved in GAD65, GadB and DDC are indicated by black arrows.

appears to be the existence and correct positioning of a negative charge in the 260–265 region. Similar conclusions can also be drawn for Lys358, the mutation of which into an asparagine residue in GAD67 was reported to completely abolish M4 monoclonal antibody binding.[20] Our model also demonstrates that the reactivity towards M8 and M9 antibodies requires amino acids from both the 134–242 region and the 532–550 region in GAD65.[20] Although in the current GAD65 model residues 129–140 are not present, several residues from the two regions are spatially contiguous. Arg177, Arg536, Glu539 and Tyr540 clearly form a single antigenic region as confirmed by the fact Arg536–Leu and Tyr540–Ser mutations are detrimental for efficient binding. Our model also concludes that Asn483 and His568 are very important for the binding of M1, M3 and M7 antibodies.[20] They define an epitope located on two helices of the small domain, one of which is the C-terminal helix. The side chains of His568 and Asn483 protrude from the C-terminus and from the other helix, respectively, and form a linear arrangement with the side chain of Tyr480, which sits between them. Lastly, our model reveals that, as reported by Tree et al.,[22] single or double replacements of Asn247 to Ser and of Leu574 to Pro produce differential effects on antibody recognition. The double replacement Asn247–Ser/Leu574–Pro results in the loss of binding for all eleven tested antibodies, while the single mutation Leu574–Pro affects the binding of some C-terminally directed antibodies (M1, M3, DP-A). On the other hand, the single mutation Asn247–Ser did not produce any effect on binding. The effect of the Leu574–Pro replacement can be structurally interpreted as perturbation of the C-terminal helix (residues 567–585), which, as mentioned above, is very important for antibody binding to the small domain. Asn247 is not spatially close to Leu574, and in the present model it can form a hydrogen bonding interaction with His362 (corresponding to His241 in GadB) (Fig. 6), a residue that has been described as critical for folding in class II decarboxylases.[49] While the Asn247–Ser replacement, which does not prevent a hydrogen bonding interaction to His362, does not destabilize the enzyme, the double mutation does indeed prevent correct folding, since it abolishes binding of all tested epitopes. A possible interpretation is that the enzyme can tolerate a minor perturbation in the large domain around the critical His362, but cannot fold if at the same time another perturbation in the C-terminal helix of the small domain is introduced.

The molecular mimicry hypothesis was also raised for GadA from *Streptococcus pneumoniae* type 3, which shares 28%/59% sequence identity/similarity to human GAD65.[50] *S. pneumoniae* GadA, for which acquisition by horizontal gene transfer was proposed,[50] aligns poorly with the prototypical bacterial glutamate decarboxylase GadB and represents a *unicum* since it does not share significant similarity to any available microbial protein [as assessed by a BLAST search against the NCBI nr database (30/04/04)]. Figure 7 shows a multiple sequence alignment of six metazoan glutamate decarboxylases (*Homo sapiens* GAD65, *H. sapiens* GAD67, *Gallus gallus* GAD67, *Danio rerio* Gad1, *Drosophila melanogaster* Gad, *Ciona intestinalis* Gad) with *S. pneumoniae* GadA. The alignment shows that many residues within the active site of GAD65 (His282, Asp 364, His 395, Lys396, Arg 558) are conserved throughout, while a difference emerges in the most N-terminal part of the seven sequences (first 100 residues of GAD65): that stretch is fully represented in the vertebrate sequences, limited to a few residues in the sea squirt and in the fruit fly sequences and absent in the *S. pneumoniae* sequence. Interestingly, the sequence of *S. pneumoniae* starts approximately where the present GAD65 model begins, at the dimer interface-enlarging domain (N-terminal domain). Secondary structure prediction with PSIPRED showed that the motif of this domain (helix-loop-short helix-loop-helix) is perfectly conserved in the *S. pneumoniae* sequence. Since GadA, though sharing a significant level of identity with GAD65, has so far been found only in one *S. pneumoniae* strain and it only partly retains the GAD65 epitopes, it is unlikely to be a candidate for molecular mimicry. The absence of the aforementioned N-terminal region in GadA suggests that this part of the sequence is only required in higher eukaryotes and likely not involved in correct folding of the protein. These conclusions are also in agreement with the finding that N-terminal truncated GAD65 (Δ1–69) is stable and active in the cell.[51]

ACKNOWLEDGMENTS

Financial support from the Swiss NCCR (Structural Biology) to M.G.G. and from the Istituto Pasteur-Fondazione Cenci Bolognetti to D.D.B. are gratefully acknowledged. The authors would like to thank Profs. Donatella Barra, Francesco Bossa and Robert John for critically reading the manuscript.

REFERENCES

1. Ueno H. Enzymatic and structural aspects on glutamate decarboxylase. J Mol Catal B: Enzymatic 2000;10(1–3):67–79.
2. Sheperd GM. The synaptic organization of the brain. New York: Oxford University Press; 1998.
3. Balcar VJ, Johnston GAR. Ontogeny of GABAergic systems in the brain. In: Redburn DA, Schousboe A, editors. GABA as a trophic agent in neuronal development. New York: Alan R. Liss; 1987. p 57–77.
4. Bowery NG, Nisticò G. GABA. Basic research and clinical applications. Rome-Milan: Pythagora Press; 1989.
5. Erdo SL, Wolff JR. gamma-Aminobutyric acid outside the mammalian brain. J Neurochem 1990;54(2):363–372.
6. Rorsman P, Berggren PO, Bokvist K, Ericson H, Mohler H, Ostenson CG, Smith PA. Glucose-inhibition of glucagon secretion involves activation of GABAA-receptor chloride channels. Nature 1989;341(6239):233–236.
7. Bosma PT, Blazquez M, Collins MA, Bishop JD, Drouin G, Priede IG, Docherty K, Trudeau VL. Multiplicity of glutamic acid decarboxylases (GAD) in vertebrates: molecular phylogeny and evidence for a new GAD paralog. Mol Biol Evol 1999;16(3):397–404.
8. Karlsen AE, Hagopian WA, Grubin CE, Dube S, Disteche CM, Adler DA, Barmeier H, Mathewes S, Grant FJ, Foster D, Lemmark A. Cloning and primary structure of a human islet isoform of glutamic acid decarboxylase from chromosome 10. Proc Natl Acad Sci U S A 1991;88(19):8337–8341.
9. Bu DF, Erlander MG, Hitz BC, Tillakaratne NJ, Kaufman DL, Wagner-McPherson CB, Evans GA, Tobin AJ. Two human glutamate decarboxylases, 65-kDa GAD and 67-kDa GAD, are each encoded by a single gene. Proc Natl Acad Sci USA 1992;89(6):2115–2119.
10. Bu DF, Tobin AJ. The exon-intron organization of the genes

(GAD1 and GAD2) encoding two human glutamate decarboxylases (GAD67 and GAD65) suggests that they derive from a common ancestral GAD. Genomics 1994;21(1):222–228.
11. Kaufman DL, Houser CR, Tobin AJ. Two forms of the gamma-aminobutyric acid synthetic enzyme glutamate decarboxylase have distinct intraneuronal distributions and cofactor interactions. J Neurochem 1991;56(2):720–723.
12. Christgau S, Schierbeck H, Aanstoot HJ, Aagaard L, Begley K, Kofod H, Hejnaes K, Baekkeskov S. Pancreatic beta cells express two autoantigenic forms of glutamic acid decarboxylase, a 65-kDa hydrophilic form and a 64-kDa amphiphilic form which can be both membrane-bound and soluble. J Biol Chem 1991;266(31): 21257–21264.
13. Reetz A, Solimena M, Matteoli M, Folli F, Takei K, De Camilli P. GABA and pancreatic beta-cells: colocalization of glutamic acid decarboxylase (GAD) and GABA with synaptic-like microvesicles suggests their role in GABA storage and secretion. Embo J 1991;10(5):1275–1284.
14. Soghomonian JJ, Martin DL. Two isoforms of glutamate decarboxylase: why? Trends Pharmacol Sci 1998;19(12):500–505.
15. Asada H, Kawamura Y, Maruyama K, Kume H, Ding RG, Kanbara N, Kuzume H, Sanbo M, Yagi T, Obata K. Cleft palate and decreased brain gamma-aminobutyric acid in mice lacking the 67-kDa isoform of glutamic acid decarboxylase. Proc Natl Acad Sci USA 1997;94(12):6496–6499.
16. Manor D, Rothman DL, Mason GF, Hyder F, Petroff OA, Behar KL. The rate of turnover of cortical GABA from [1-13C]glucose is reduced in rats treated with the GABA-transaminase inhibitor vigabatrin (gamma-vinyl GABA). Neurochem Res 1996;21(9):1031–1041.
17. Martin DL, Rimvall K. Regulation of gamma-aminobutyric acid synthesis in the brain. J Neurochem 1993;60(2):395–407.
18. Baekkeskov S, Kanaani J, Jaume JC, Kash S. Does GAD have a unique role in triggering IDDM? J Autoimmun 2000;15(3):279–286.
19. Baekkeskov S, Landin M, Kristensen JK, Srikanta S, Bruining GJ, Mandrup-Poulsen T, de Beaufort C, Soeldner JS, Eisenbarth G, Lindgren F, Sundquist G, Lemmark A. Antibodies to a 64,000 Mr human islet cell antigen precede the clinical onset of insulin-dependent diabetes. J Clin Invest 1987;79(3):926–934.
20. Schwartz HL, Chandonia JM, Kash SF, Kanaani J, Tunnell E, Domingo A, Cohen FE, Banga JP, Madec AM, Richter W, Baekkeskov S. High-resolution autoreactive epitope mapping and structural modeling of the 65 kDa form of human glutamic acid decarboxylase. J Mol Biol 1999;287(5):983–999.
21. Tong JC, Myers MA, Mackay IR, Zimmet PZ, Rowley MJ. The PEVKEK region of the pyridoxal phosphate binding domain of GAD65 expresses a dominant B cell epitope for type 1 diabetes sera. Ann N Y Acad Sci 2002;958:182–189.
22. Tree TI, Morgenthaler NG, Duhindan N, Hicks KE, Madec AM, Scherbaum WA, Banga JP. Two amino acids in glutamic acid decarboxylase act in concert for maintenance of conformational determinants recognised by Type I diabetic autoantibodies. Diabetologia 2000;43(7):881–889.
23. Myers MA, Davies JM, Tong JC, Whisstock J, Scealy M, Mackay IR, Rowley MJ. Conformational epitopes on the diabetes autoantigen GAD65 identified by peptide phage display and molecular modeling. J Immunol 2000;165(7):3830–3838.
24. Syren K, Lindsay L, Stoehrer B, Jury K, Luhder F, Baekkeskov S, Richter W. Immune reactivity of diabetes-associated human monoclonal autoantibodies defines multiple epitopes and detects two domain boundaries in glutamate decarboxylase. J Immunol 1996; 157(11):5208–5214.
25. Solimena M, Folli F, Denis-Donini S, Comi GC, Pozza G, De Camilli P, Vicari AM. Autoantibodies to glutamic acid decarboxylase in a patient with stiff-man syndrome, epilepsy, and type I diabetes mellitus. N Engl J Med 1988;318(16):1012–1020.
26. Chattopadhyay S, Ito M, Cooper JD, Brooks AI, Curran TM, Powers JM, Pearce DA. An autoantibody inhibitory to glutamic acid decarboxylase in the neurodegenerative disorder Batten disease. Hum Mol Genet 2002;11(12):1421–1431.
27. Qu K, Martin DL, Lawrence CE. Motifs and structural fold of the cofactor binding site of human glutamate decarboxylase. Protein Sci 1998;7(5):1092–1105.
28. Burkhard P, Dominici P, Borri-Voltattorni C, Jansonius JN, Malashkevich VN. Structural insight into Parkinson's disease treatment from drug-inhibited DOPA decarboxylase. Nat Struct Biol 2001;8(11):963–967.
29. Capitani G, De Biase D, Aurizi C, Gut H, Bossa F, Grutter MG. Crystal structure and functional analysis of *Escherichia coli* glutamate decarboxylase. Embo J 2003;22(16):4027–4037.
30. Jones TA, Kjeldgaard M. Manual for O. 5.6. Uppsala, Sweden: Uppsala University; 1991.
31. Devereux J, Haeberli P, Smithies O. A comprehensive set of sequence analysis programs for the VAX. Nucleic Acids Res 1984;12(1 Pt 1):387–395.
32. Cuff JA, Clamp ME, Siddiqui AS, Finlay M, Barton GJ. JPred: a consensus secondary structure prediction server. Bioinformatics 1998;14(10):892–893.
33. Sali A. Comparative protein modeling by satisfaction of spatial restraints. Mol Med Today 1995;1(6):270–277.
34. Laskowski RA, MacArthur MW, Moss DS, Thornton JM. PROCHECK: a program to check the stereochemical quality of protein structure. J Appl Cryst 1993;26:283–291.
35. Brünger AT. X-PLOR manual, vers. 3.1. New Haven, CT: Yale University; 1992.
36. Hooft RW, Vriend G, Sander C, Abola EE. Errors in protein structures. Nature 1997;381:272.
37. Grishin NV, Phillips MA, Goldsmith EJ. Modeling of the spatial structure of eukaryotic ornithine decarboxylases. Protein Sci 1995;4(7):1291–1304.
38. Jones DT. Protein secondary structure prediction based on position-specific scoring matrices. J Mol Biol 1999;292(2):195–202.
39. Kanaani J, el-Husseini Ael D, Aguilera-Moreno A, Diacovo JM, Bredt DS, Baekkeskov S. A combination of three distinct trafficking signals mediates axonal targeting and presynaptic clustering of GAD65. J Cell Biol 2002;158(7):1229–1238.
40. Jansonius JN. Structure, evolution and action of vitamin B6-dependent enzymes. Curr Opin Struct Biol 1998;8(6):759–769.
41. Chen CH, Wu SJ, Martin DL. Structural characteristics of brain glutamate decarboxylase in relation to its interaction and activation. Arch Biochem Biophys 1998;349(1):175–182.
42. Chen CH, Battaglioli G, Martin DL, Hobart SA, Colon W. Distinctive interactions in the holoenzyme formation for two isoforms of glutamate decarboxylase. Biochem Biophys Acta 2003;1645(1):63–71.
43. Baekkeskov S, Aanstoot HJ, Christgau S, Reetz A, Solimena M, Cascalho M, Folli F, Richter-Olesen H, De Camilli P, Camilli PD. Identification of the 64K autoantigen in insulin-dependent diabetes as the GABA-synthesizing enzyme glutamic acid decarboxylase. Nature 1990;347(6289):151–156.
44. Bjork E, Velloso LA, Kampe O, Karlsson FA. GAD autoantibodies in IDDM, stiff-man syndrome, and autoimmune polyendocrine syndrome type I recognize different epitopes. Diabetes 1994;43(1): 161–165.
45. Roep BO, Atkinson MA, van Endert PM, Gottlieb PA, Wilson SB, Sachs JA. Autoreactive T cell responses in insulin-dependent (Type 1) diabetes mellitus. Report of the first international workshop for standardization of T cell assays. J Autoimmun 1999;13(2):267–282.
46. Roep BO, Hiemstra HS, Schloot NC, De Vries RR, Chaudhuri A, Behan PO, Drijfhout JW. Molecular mimicry in type 1 diabetes: immune cross-reactivity between islet autoantigen and human cytomegalovirus but not Coxsackie virus. Ann NY Acad Sci 2002;958:163–165.
47. Momany C, Ernst S, Ghosh R, Chang NL, Hackert ML. Crystallographic structure of a PLP-dependent ornithine decarboxylase from Lactobacillus 30a to 3.0 Å resolution. J Mol Biol 1995;252(5): 643–655.
48. Myers MA, Fenalti G, Gray R, Scealy M, Tong JC, El-Kabbani O, Rowley MJ. A diabetes-related epitope of GAD65: a major diabetes-related conformational epitope on GAD65. Ann NY Acad Sci 2003;1005:250–252.
49. Capitani G, Tramonti A, Bossa F, Grutter MG, De Biase D. The critical structural role of a highly conserved histidine residue in group II amino acid decarboxylases. FEBS Lett 2003;554(1–2):41–44.
50. Garcia E, Lopez R. *Streptococcus pneumoniae* type 3 encodes a protein highly similar to the human glutamate decarboxylase (GAD65). FEMS Microbiol Lett 1995;133(1–2):113–118.
51. Wei J, Jin Y, Wu H, Sha D, Wu JY. Identification and functional analysis of truncated human glutamic acid decarboxylase 65. J Biomed Sci 2003;10(6 Pt 1):617–624.
52. Thompson JD, Gibson TJ, Plewniak F, Jeanmougin F, Higgins DG. The CLUSTAL_X windows interface: flexible strategies for multiple sequence alignment aided by quality analysis tools. Nucleic Acids Res 1997;25(24):4876–4882.